Sustainable Energy Research

RESEARCH

Open Access

Modeling, design and optimization of integrated renewable energy systems for electrification in remote communities

Kuanrong Qiu[1*] and Evgueniy Entchev[1]

Abstract

Integrated renewable energy systems are becoming a promising option for electrification in remote communities. Integrating multiple renewable energy sources allows the communities to counteract the weaknesses of one renewable energy source with the strengths of another. This study aims to model, design and optimize integrated renewable energy systems consisting of solar photovoltaic (PV) panels, wind turbines, a biomass power generator, and storage batteries for applications in remote communities in Canada. Biomass is used as a fuel to produce electricity during periods when solar power and wind power are not capable of meeting the power demand. A methodology is developed to optimize the integrated renewable energy systems design, with the aim of minimizing the net present cost (NPC) and the levelized cost of electricity (LCOE) of the energy systems. Results show that the NPC is $3.61 M and the LCOE is $0.255/kWh for an optimized integrated renewable energy system in a sample remote community that has a peak power consumption of 238.7 kW and an average load demand of 2230 kWh/day. Through the present research, the integrated energy systems are evidenced to be an effective option for electrification in remote communities.

Keywords Integrated renewable energy systems, Levelized cost of electricity, Remote communities, Economic assessment, Energy system modeling

Introduction

There are several factors that have attracted significant attention to renewable energy applications. The factors include advancing renewable energy technologies, growing environment concerns, and interest towards energy sustainability and security. Although renewable energy utilization is important to sustainable development, certain issues such as the intermittent nature of solar and wind generation and production costs are to be considered in the design and application of the renewable energy systems. The intermittency issue can be overcome by using integrated renewable energy systems where two or more types of renewable energy sources are integrated. In other words, combining multiple renewable energy sources including solar, wind and biomass can offset each other's weaknesses. The costs of electricity production could be reduced by optimizing the integrated energy systems according to geographical places. Hence, the optimization of integrated renewable energy systems is a research field with important areas worthy to be investigated (Bahramara et al., 2016; Prabatha et al., 2020). Suitable methodologies can provide simulation support tools for system sizing at the project design stages and evaluation of trade-offs among various system configurations (Kamaril et al., 2020; Thirunavukkarasu et al., 2023). For instance, economic sizing of an integrated renewable energy system for stand-alone usage was analyzed by Hosseinalizadeh et. al. (2016). They

*Correspondence:
Kuanrong Qiu
kuanrong.qiu@nrcan-rncan.gc.ca
[1] Natural Resources Canada, CanmetENERGY Technology Centre, 1 Haanel Drive, Ottawa, ON K1A 1M1, Canada

simulated the performance of various renewable energy system configurations incorporating solar photovoltaic (PV) cells, wind turbine and fuel cell (FC) for use in Iran. Bagheri et. al. (2018) examined optimal planning of integrated renewable energy infrastructure for urban sustainability and assessed the impact of the economics of scale on the life-cycle costs of hybrid renewable systems for Vancouver, Canada. Akinyele and Rayudu (2016) conducted techno-economic and environmental analyses of a solar PV microgrid for remote communities in a small village. Shahzad et. al. (2017) proposed an optimal economic plan for electricity generation using an integrated renewable energy system, including solar panels and biomass on an agricultural field and a residential community in Pakistan. Shezan et. al. (2016) examined an off-grid integrated energy system consisting of solar PV, wind turbine, diesel power and batteries for a small community in Malaysia with an average load demand of 33 kWh/day and a peak load of 3.9 kW to reduce dependence on fossil fuels. Their research showed that the net present cost (NPC) of the designed integrated energy system was 29.7% less than the NPC of the conventional power plant. Baneshi and Hadianfard (2016) investigated the viability of generating electricity from an energy system including batteries, diesel generator, solar cells and wind turbine, noting that adding battery component to the stand-alone integrated energy system improved overall system efficiency.

The process of selecting a proper integrated energy system could be a complex task. Sedghiyan et. al. (2021) noted that the most suitable renewable energy sources in Iran were solar and then wind energy. In fact, solar and wind power production technologies are used in many countries due to their maturity, high social acceptance, and widespread use (Almutairi et al., 2021). However, the use of a single renewable energy source such as wind or solar energy to supply electricity has low reliability due to the availability of these sources being intermittent or random and dependent on weather conditions (Sameti et al., 2014). Therefore, combining renewable sources to form an integrated energy system is an effective solution to overcoming the weaknesses of a single renewable energy source (Sinha et al., 2014). Singh et. al. (2016) carried out a feasibility study of a renewable energy based microgrid in rural area and used a swarm based artificial bee colony algorithm to optimize the sizing of system components. Comparably, Diab et. al. (2020) studied optimal sizing of hybrid solar/wind/hydroelectric pumped storage energy system in Egypt based on different metaheuristic techniques. They investigated the implementation of different optimization techniques to achieve optimal sizing of grid-connected hybrid renewable energy systems. Also, Rahbar et. al. (2018) studied energy cooperation optimization in microgrids with renewable energy integration and the impacts of microgrids' energy cooperation and energy storage on electricity cost. Bartolini et. al. (2020) investigated multi-energy systems with energy storage for local communities and evaluated the optimal portfolio of energy conversion and lithium-ion battery electricity storage, but they did not disclose the cost of the battery. More recently, Afif et al. (2023) have carried out a feasibility and optimal sizing analysis of hybrid renewable energy systems. In their case study, grid-connected and stand-alone renewable energy systems consist of a wind turbine, a biogas power plant, solar PV panels, flywheels, and batteries. They claimed that a cost of electricity of \$0.049 kWh could be achieved by the hybrid energy systems.

Mahbaz et. al. (2020) evaluated the needs and requirements for the provision of critical energy services to communities in Canada's northern regions. They proposed enhanced geothermal system concepts as part of integrated solutions over the long term and conducted a technical and economic feasibility study of the integration of different local energy sources (renewable and non-renewable) to establish a pathway for low-carbon and sustainable energy supply. Moreover, Das and Cañizares (2019) examined renewable energy integration in diesel-based microgrids in Canada's remote arctic communities where the dependence on diesel and its associated costs are an economic issue and found that the optimal plan was diesel–renewable hybrid combinations. In parallel, Holdmann et. al. (2019) analyzed economic drivers and technical strategies for renewable energy integration in Alaska's remote islanded microgrids and pointed out that the primary technical hurdles for renewable energy integration included management of distributed energy resources and reliable design for resilient operation. Holdmann et. al. (2022) discussed pathways to renewable energy transitions in remote Alaska communities where climate conditions are more or less similar to communities in Northern Canada. These researchers conducted a comparative analysis of 24 remote communities in Alaska to identify the factors that could lead to implementing renewable energy technologies and showed that three most important primary factors were community capacity to manage projects and infrastructure, electricity subsidies, and pooled resources. McCallum et. al. (2021) examined renewable electricity generation for off-grid remote communities in Alaska and compared the renewable electricity generation with the existing diesel electricity generation based on a life-cycle assessment. Their comparative results showed that the transition from diesel electricity generation could reduce the carbon intensity of energy generation from 1345.46 to 175.56 kg CO_2/MWh. Recently, Sambor et. al. (2023)

have analyzed and optimized a 25-kW microgrid system consisting of solar PV panels, batteries and a diesel power generator in Yukon, Canada, to determine how to best operate the diesel generator to maximize solar PV generation, thus minimizing diesel cost. They reported that solar PV with batteries could meet 96% of load during June, but only 3% during December, and 67% year-round. However, no information on battery cost was provided in their paper. Also, Stringer and Joanis (2023) have used an integer optimization model to analyze the least costly decarbonization solution for Canada's remote microgrids from now until 2050. Their analysis results show that the cost of decarbonizing Canada's remote microgrids is not prohibitive. Wind turbines appeared to be the cheapest option for many examined off-grid communities in 2020, whereas solar PV would be the cheapest option in the future. They have noted that communities that currently use diesel to produce electricity should consider undergoing decarbonization as soon as possible.

Canada has approximately ten million square-kilometers of land, and expanding the electrical grid to every corner of the country is not financially feasible. As a result, there are more than 300 communities including many remote aboriginal ones across Canada where people live off-grid (Government of Canada, 2011). In these communities, fossil fuel-based generators are a commonly adopted source of electricity generation, resulting in adverse environmental impacts. Investigations of optimized integrated renewable energy systems at community-scale, are therefore required, especially under the conditions of Canada's remote northern communities, most of which are dependent on diesel power.

The main objective of this study is to model, design and optimize integrated renewable energy systems for remote community applications in Canada, with the aim of replacing diesel power in the areas where diesel fuel is being used for electricity production. This paper presents a methodology for designing, optimizing, and ranking the integrated energy systems. The optimized system configuration can minimize the NPC as well as the levelized cost of electricity (LCOE). The optimization is performed using the HOMER software (HOMER Energy, 2023).

Integrated renewable energy systems

Description

The design of integrated renewable energy systems involves modular arrangement for solar PV and wind turbine units to obtain the required capacity by increasing or decreasing the number of solar PV panels and wind turbines. The system size is optimized through determination of the number of solar PV panels and wind turbines. The biomass to power module consists of a biomass gasifier and an internal combustion engine (ICE) generator. The integrated renewable energy systems are designed by prioritizing solar and wind power subsystems over the biomass to power subsystem. The integrated system power capacity is determined using the established model based on the average value of hourly power demand of the selected community.

System components

Solar PV panel

Solar PV is widely used to produce electric power from sunlight. The power output of PV panels is affected by various parameters such as solar irradiation, cell efficiency, daytime ambient temperature, etc. In practice, the solar PV performance depends on the cell technology, geographical location, tilt angle and dust accumulation on the solar PV panels. The power output of a solar PV panel is calculated from (Almutairi et al., 2021; Jahangiri et al., 2019):

$$P_{\mathrm{PV}} = P_0 f_{\mathrm{PV}} \frac{I_{\mathrm{T}}}{I_{\mathrm{S}}} [1 + \alpha (T_{\mathrm{C}} - T_{\mathrm{S}})], \quad (1)$$

where P_0 is the nominal power of the solar PV panel, f_{PV} is the derating factor relative to the losses due to soiling on the panel and the ambient temperature effect, I_{T} is the incident radiation (kW/m^2), I_{S} is the incident radiation on the cell surface under standard conditions (1 kW/m^2), α is the temperature coefficient, T_{C} is the cell temperature under operating conditions, and T_{S} is the temperature of cells under standard test conditions. There are different models for solar PV power generation, resulting in different calculation formulae (Hoff & Perez, 2010). Equation (1) was derived and used by many researchers (Dolara et al., 2015; IEC, 2021).

Figure 1 shows the daily horizontal radiation and clearness index over a year at the study location that is in Canada's Inuvik region (NASA, 2017). The clearness index is a measure of the clearness of the atmosphere and is

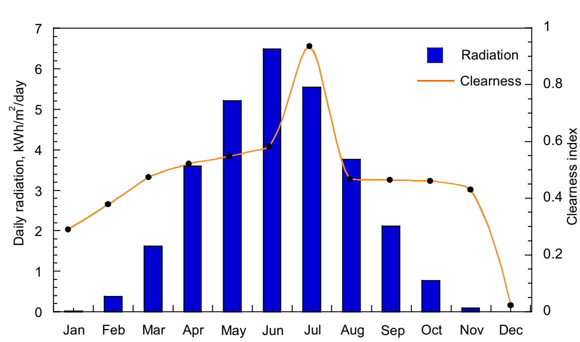

Fig. 1 Daily horizontal radiation and clearness index for 12 months at the study location

defined as the surface radiation divided by the extraterrestrial radiation.

Wind turbine

The amount of air entering and exiting a turbine is unchanged due to the mass conservation of the air stream. Based on Betz's law (Hansen, 2007), the maximal achievable extraction of wind power by a wind turbine equals 16/27% of the kinetic energy of the air that reaches the effective disk area of the turbine equipment. Here, it is noted that Betz' law is a theory about the maximum possible energy to be derived from a wind turbine. It was developed in 1919 by German physicist Albert Betz. According to the rule, no turbine can capture more than 59.3 (16/27) % of the potential energy in wind. Thus, the maximum power output, P_{wm} of a turbine is given by (Solomon et al., 2023):

$$P_{\mathrm{wm}} = 8\rho v A/27, \tag{2}$$

where A is the effective area of the disk, v is the wind velocity, and ρ is the air density. The rated power of the wind turbine is obtained from:

$$P_{\mathrm{wr}} = 8\rho v A\ C_{\mathrm{wp}}/27, \tag{3}$$

where C_{wp} is the power coefficient provided by a manufacturer. In addition, the power output of the wind turbine varies with the hub height. At a given hub height H, the wind velocity is calculated from (Baghaee et al., 2016):

$$v = v_{\mathrm{ref}}\left(\frac{H}{H_{\mathrm{ref}}}\right)^{\gamma}, \tag{4}$$

where v_{ref} is the reference velocity measured at the reference hub height, H_{ref} is the reference hub height and γ is the power law exponent or Hellmann exponent (Tar, 2008). It is in range of 0.10 to 0.25. A power law exponent value of 0.15 is used in the present work. Figure 2 shows the monthly average wind velocities at a reference hub height of 10 m at the study location, with the annual average being 5.3 m/s (NASA, 2017). A wind turbine with rated 10 kW capacity is chosen for the present case study.

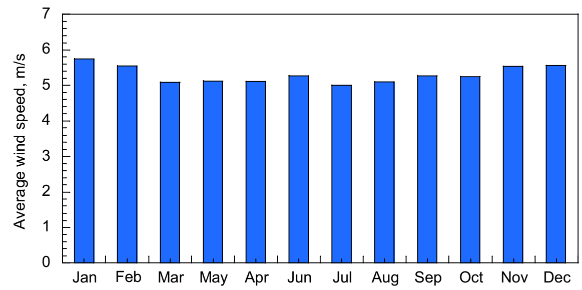

Fig. 2 Monthly average wind velocities at a reference hub height of 10 m at the study location

Biomass power

Biomass to power is achieved using a biomass gasifier together with an ICE generator. Biomass gasification comprises an incomplete biomass combustion process at high temperatures, resulting in the production of combustible gases. The produced biogas can have a lower heating value (LHV) of approximate 5.5 MJ/kg (Bagheri et al., 2018; Couto et al., 2013) and be used as a fuel in ICE or more efficient gas turbines. Note that 1 kg of wood biomass can produce 2.4 kg of biogas from the gasification. The LHV of the biomass is relatively low due to high CO_2 and N_2 content (Couto et al., 2013). In this study, the biogas LHV calculated using HOMER is 5.5 MJ/kg as well. The net power output from a biogas-fired generator is expressed as (Bagheri et al., 2018):

$$P_{\mathrm{bioel}} = P_{\mathrm{bio\_tot}} - P_{\mathrm{aux}} = \eta_{\mathrm{bioel}} G_{\mathrm{LHV}} V_{\mathrm{bio}}, \tag{5}$$

where $P_{\mathrm{bio\_tot}}$ is the total electrical output, P_{aux} is the power needed for auxiliary components, η_{bioel} is the electric conversion efficiency, G_{LHV} is the lower heating value of biogas, and V_{bio} is the volumetric flow rate of biogas.

Batteries

In integrated energy systems, the incorporation of batteries increases system reliability (Bagheri et al., 2018). The batteries serve as energy storage medium, store surplus renewable energy, and supply the energy during capacity shortage. At present, the estimated cost for the suggested lithium-ion batteries is $550/kWh for remote community applications (HOMER Energy, 2023). The simulations are performed in increments of 100 kWh for battery energy storage capacity, in accordance with the chosen battery size per pack. It is known that lithium-ion battery price has decreased significantly over the past decade and the price is expected to decrease further as the battery technology progresses. The integrated renewable energy systems are proposed and designed for the remote northwestern communities in Canada where expensive and carbon-intensive diesel power is consumed. Table 1 shows the capital, replacement, and O&M costs for solar PV, wind turbine, biomass to power and battery components, and associated technical characteristics.

Economic assessment

LCOE and NPC are considered the most relevant economic indicators and the achievement of their minimum values defines an optimal energy system. The real interest rate is calculated from (Dehshiri, 2022):

Table 1 Economic and technical characteristics of system components

Component characteristics	Biomass gasifier-ICE generator	Solar PV panel	Wind turbine	Converter	Battery
Specific capital cost ($)	4500/kW	1000/kW	20,000/10 kW unit	150/kW	550/kWh
Replacement cost ($)	3500/kW	1000/kW	16,000/10 kW unit	150/kW	550/kWh
O&M cost ($)	525/kW/yr	20/kW/yr	500/unit/yr	20/kW/yr	10/kW/yr
Efficiency (%)	35	17	40	90	90
Nominal power	270 kW	250W/panel	10 kW/unit	10 kW/unit	N/A[a]
Lifetime (years)	20	20	20	20	10

[a] Battery nominal capacity: 100 kWh/pack

$$i = \frac{i' - f}{i' + f}, \tag{6}$$

where i' is the nominal interest rate and f is the rate of annual inflation. NPC is calculated from:

$$\text{NPC} = \frac{C_{\text{atot}}}{\text{CRF}\ (i, N)}, \tag{7}$$

where C_{atot} is the total annualized cost, *CRF* is the capital recovery factor and N is the project lifetime. CRF is given by:

$$\text{CRF}\ (i, N) = \frac{i(1+i)^N}{(1+i)^N - 1}, \tag{8}$$

LCOE, i.e., the price of each kilowatt hour of electricity generated, is calculated from (Branker et al., 2011):

$$\text{LCOE} = \frac{C_{\text{atot}}}{E_{\text{load}}}, \tag{9}$$

where E_{load} is the total electrical load served annually (kWh/year). LCOE is used to evaluate the economic competitiveness of electricity generation technologies over the long term (Branker et al., 2011).

System modeling

The proposed integrated renewable systems consist of solar PV, wind turbine, biomass-based generator, and electricity storage unit. The biomass-based generator supplies power on demand when solar PV and wind turbine are not capable of meeting required power demand. HOMER is used to simulate the integrated power systems performance and optimize integrated system configurations. The HOMER built-in algorithm performs calculations of hourly power balance for predefined integrated scenarios subject to meeting multi-criteria and constraints. It uses the load demand profile, the resources, the component specifications, the constraints, and the emission data as inputs to simulate various feasible configurations and rank them. Table 2 lists the constraints used in the optimization process.

Table 2 Constraints for HOMER optimization procedure

Parameter	Value
Annual capacity shortage (%)	0
Hourly load operating reserve (%)	10
Penalties over CO_2 emissions ($/ton)	0
Project lifetime (years)	20
Minimum renewable fraction (%)	100
Discount rate (%)	6.5%
Inflation rate (%)	5%

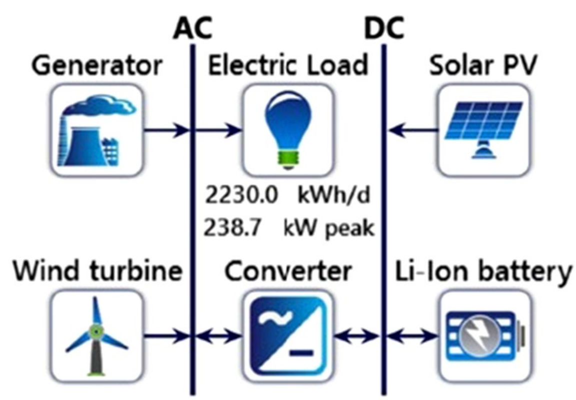

Fig. 3 Schematic of the proposed integrated renewable energy system

Figure 3 shows the model schematic of the integrated renewable energy system. The components of the integrated energy system include solar PV, wind turbine, biomass-based generator, battery, and converter (HOMER Energy, 2023). Figure 4 illustrates the flow diagram of the modeling and optimization procedure used in this study. Specifically, economic data, load data, technical data, environmental data such as equivalent CO_2 emission factors of the components

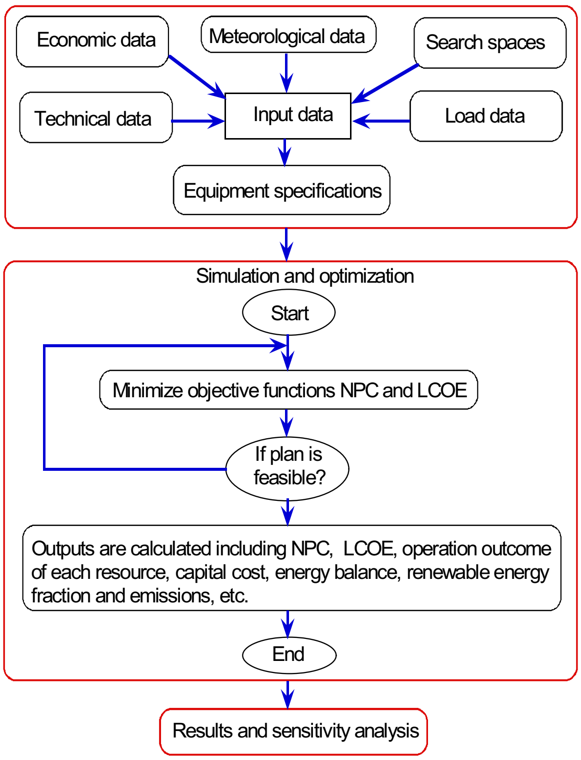

Fig. 4 HOMER simulation and optimization procedure

and hourly time step are used to seek optimal system configurations.

The objective functions in the optimization are based on minimum NPC and LCOE. NPC of a power system is defined as the system's present value costs over the system lifetime minus the net present value of all the revenues that it earns over the system lifetime (Chauhan & Saini, 2016). NPC is calculated from Eq. (7) and LCOE is calculated from Eq. (9) (HOMER Energy, 2023). Optimum system configurations are displayed after the simulation is completed using a wide variety of tables and graphs to compare and evaluate them according to their economic and technical merits (Anoune et al., 2018).

Results and discussion

Electric load in the sample community

One remote northwestern community in Inuvik region, Canada, has been selected for the present case study. The sample community has an average load demand of 2230 kWh/day (813,950 kWh/year), and its peak power consumption is 238.7 kW. Electric load time series data were collected using power meters. The data include apparent power, active power, and voltage. Daily load profiles were extracted from the collected time series data and served as input dataset for simulation. Figure 5 shows the daily profile of the electric load on a typical day

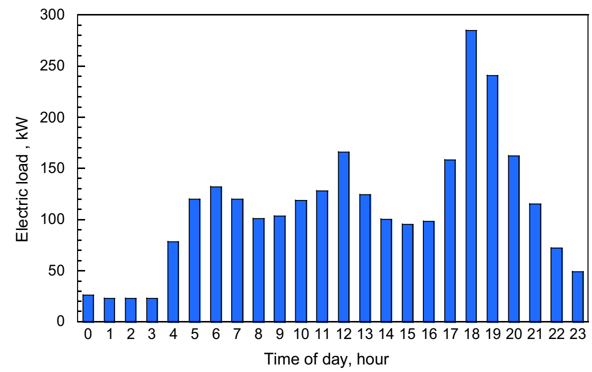

Fig. 5 Daily profile of electric load in the sample community

at the sample community. The daily cycle of electricity demand begins in the early morning when people wake up and start getting ready for the day. Electricity demand generally peaks between 5 and 8 p.m. As nighttime approaches, electricity consumption slows before repeating the cycle on the following day. Figure 6 shows the seasonal profile of the electric load.

System configuration and economics

Different configuration scenarios of integrated renewable energy systems have been designed and optimized for the sample community. Table 3 presents the results of the top two optimized configurations. The configuration scenarios are ranked according to their NPC and LCOE. The obtained NPC and LCOE are \$3.61 M and \$0.255/kWh for scenario 1, and the obtained NPC and LCOE are \$3.66 M and \$0.262/kWh for scenario 2. These two scenarios have lowest NPCs and LCOEs, as opposed to others assessed, while being capable of satisfying the peak power load demand of the sample community.

Based on the simulation results, the total electricity production by the integrated energy system Scenario 1 is 883,090 kWh/year and the electricity production by the integrated energy system Scenario 2 is 864,193 kWh/year. Thus, the designed energy systems can meet the

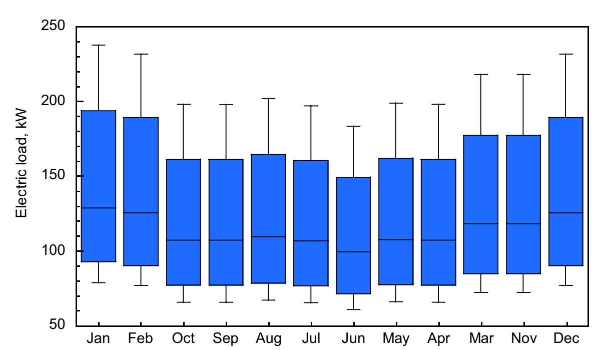

Fig. 6 Seasonal profile of electric load in the sample community

Table 3 Optimized integrated renewable energy systems for the sample community

Case	System component					Cost				
	Biomass to power (kW)	Solar PV panel (kW)	Wind turbine (kW)	Converter (kW)	Battery (kWh)	Biomass ($/dry ton)	Capital cost (M$)	O&M ($/yr.)	NPC (M$)	LCOE ($/kWh)
Scenario 1	270	80	130	210	600	45	1.89	101,288	3.61	0.255
Scenario 2	270	50	110	160	500	45	1.78	106,986	3.66	0.262

community's total electric energy demand. Table 4 presents the breakdown of electricity production and LCOE from the renewable sources for the two scenarios. For Scenario 1, the biomass-based electricity, the electricity produced from solar PV panels and the electricity produced from wind turbines account for 61.2%, 8.08% and 30.7%, respectively. For Scenario 2, the biomass-based electricity, the electricity produced from solar PV panels and the electricity produced from wind turbines account for 68.3%, 5.15% and 26.5%. For both scenarios, the biomass power generator is the primary energy source in the entire energy system. The capital cost and the LCOE of each component in the integrated energy systems are also presented in Table 4.

Figure 7 shows the power output distribution of the solar PV panels with 80 kW rated capacity over a year for Scenario 1. Obviously, electricity is generated during the daytime and little electricity is generated during the winter season. Their mean electricity production is 195 kWh/day, and the total electricity production is 71,321 kWh/year. It is noted that for Scenario 2, the solar PV power output distribution pattern is the same as that of Scenario 1, yet the mean electricity production is 122 kWh/day, and the total electricity production is 44,782 kWh/year. On the other hand, the LCOE from solar PV is the same for both scenarios ($0.087/kWh), which turns out to be independent of the system configurations but is determined by local radiation conditions and solar cell efficiency. Solar PV has the advantages of low operational and maintenance costs. However, it has intermittent characteristics, as shown in Fig. 7.

Figure 8 illustrates the power output distribution of the wind turbines with 130 kW rated capacity for 365 days for Scenario 1. The mean electricity production of the wind turbines is 724 kWh/day, and their total electricity production is 271,036 kWh/year. As to Scenario 2, the pattern of the power output distribution of wind turbines is similar to what is shown in Fig. 8, but their mean electricity production is reduced to 623 kWh/day, and their total electricity production is reduced to 229,339 kWh/year. For both scenarios, the LCOE is the same (Table 4), the capacity factor of the wind turbines is 23.6%, and the hours of their operation are 7189 h/year in the sample community. In addition, it is observed that the solar power and wind power are consistent with the available solar and wind resources.

Here, it is worth noting that renewable integration can be a critical element of a net-zero future, which will reduce reliance on fossil fuels and lower carbon emissions, resulting in far-reaching benefits for society. In other words, integrating renewable energy sources is among the key strategies that can address climate change while accelerating the transition to a green economy. Canada has been committed to clean electricity in more than 200 remote communities that still depend on carbon-intensive diesel power by 2035. The results presented above show that the proposed integrated renewable energy systems can well satisfy the electric energy demand of the studied community, and the LCOE appears to be attractive for electrification in remote communities although carbon credit has not been considered (Lovekin & Heerema, 2019). The results of this study would help support the decision-making regarding the adoption of the clean energy technologies and energy transitions.

Sensitivity analysis

A sensitivity analysis can assess which variables have the greater impact on the economic indicator NPC of a power system. Table 5 shows the results of the sensitivity analysis. The analysis has been conducted by changing the values of the variables independently. It is observed that an increase in component costs, inflation rate and biomass price leads to increases in the NPC but to different extents. For instance, a 20% increase in biomass-based generator capital cost gives rise to 4.98% and 6.75% increases in the NPC for Scenarios 1 and 2, respectively, while a 20% increase in the capital costs of solar PV panel, wind turbine and battery bring about relatively less increases in the NPC.

On the other hand, the increase in discount rate and conversion efficiencies leads to decreasing the NPC. A 20% rise in discount rate results in quite a significant decrease in the NPC, with the NPC variations being −7.32% and −6.14% for Scenarios 1 and 2, respectively. The implication is that the discount rate on capital

Table 4 Breakdown of electricity production and LCOE from the renewable sources for the top two optimized scenarios

Case	Biomass-based generator				Solar PV panel				Wind turbine			
	Electricity production		Capital cost (M$)	LCOE ($/kWh)	Electricity production		Capital cost ($)	LCOE ($/kWh)	Electricity production		Capital cost ($)	LCOE ($/kWh)
Scenario 1	540,726 kWh/yr	61.2%	1.215	0.301	71,321 kWh/yr	8.08%	80,000	0.087	271,036 kWh/yr	30.7%	260,000	0.079
Scenario 2	590,275 kWh/yr	68.3%	1.215	0.308	44,580 kWh/yr	5.15%	50,000	0.087	229,338 kWh/yr	26.5%	220,000	0.079

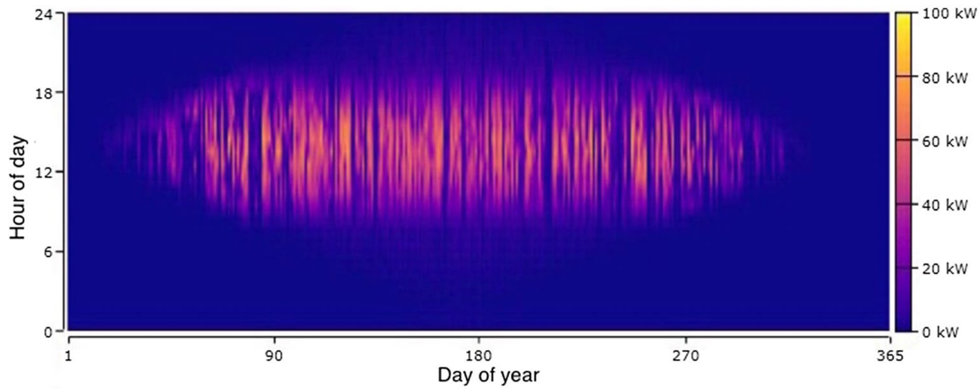

Fig. 7 Power output distribution of the solar PV panels with 80 kW rated capacity at the sample location for 365 days. Hours of operation: 3615 h/year

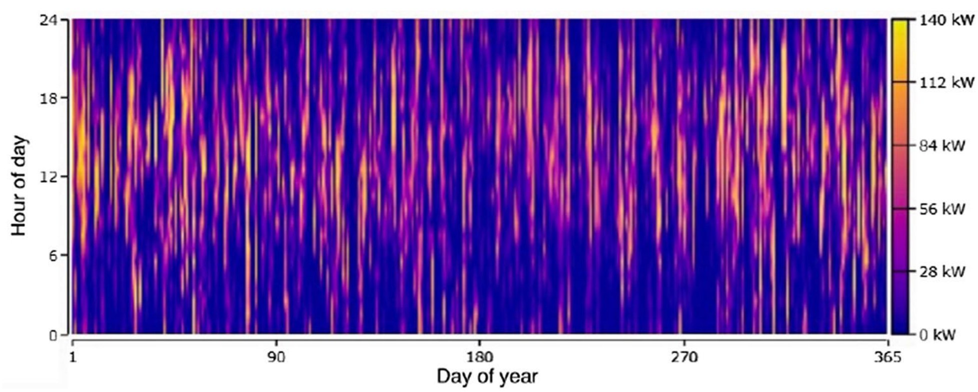

Fig. 8 Power output distribution of the wind turbines with 130 kW rated capacity days at the sample location for 365. Hours of operation: 7189 h/year

Table 5 Sensitivity analysis of key variables

Variable	Scenario 1		Scenario 2	
	Variation (%)	Change in NPC (%)	Variation (%)	Change in NPC (%)
Solar PV capital cost	20	0.31	20	0.4
Biomass-based generator capital cost	20	4.98	20	6.75
Wind turbine capital cost	20	1.35	20	1.03
Discount rate	20	− 7.32	20	-6.14
Inflation rate	20	6.13	20	4.97
Biomass price	20	1	20	1.25
Battery capital cost	20	2.49	20	2.32
Biomass-based generator efficiency	10	− 1.51	10	− 1.62
Wind turbine efficiency	10	− 1.38	10	− 1.25
Solar PV panel efficiency	10	− 1.23	10	− 1.02

investment has the greater impact on the economic viability of the renewable energy systems. In contrast, the same rise in inflation rate leads to the positive NPC variations of 6.13% and 4.97% for the two configurations. Moreover, Table 5 shows that the increase in the existing efficiency of biomass-based generator, wind turbine or solar PV panel by 10% results in an NPC change of − 1.23% to − 1.51% for Scenario 1, and an NPC change of − 1.02% to − 1.62% for Scenario 2. This suggests that any efficiency improvements in the renewable energy technologies will reduce the NPC of an integrated renewable energy system and thus increase the economic competitiveness of the integrated energy system.

Conclusions

Combining solar PV, wind turbine, biomass-based generator and battery can constitute integrated renewable energy systems for applications in Canada's remote communities. The integrated energy systems are investigated and shown to be a strong solution to supply clean electricity to the communities through the case study. Integrating multiple renewable energy sources counteracts the weaknesses of one stochastic renewable energy source with the strengths of another. The developed methodology is proven to be effective and useful in the design and optimization of integrated renewable energy systems. Different system configurations consisting of solar PV panels, biomass-based generator, wind turbines and batteries are designed and optimized for electrification in a remote sample community. The obtained results show that for the top two optimized design scenarios, the biomass-based electricity accounts for 61.2% and 68.3% of the total electricity produced by the integrated energy systems, the electricity produced from solar PV panels accounts for 8.08% and 5.15%, and the electricity produced from wind turbines accounts for 30.7% and 26.5%, respectively. The capacity value of the biomass power generator is 270 kW in the two chosen optimized system scenarios, while the capacity values of solar PV panels are 80 kW and 50 kW and wind turbines are 130 kW and 110 kW, respectively. The proposed energy systems effectively satisfy the electric energy demand of the remote northwestern community while their NPC and LCOE are minimized. The sensitivity analysis reveals that increases in discount rate and conversion efficiencies result in a decrease in the NPC, whereas increases in the component costs, inflation rate and biomass price result in an NPC increase. It is found that the variations in biomass to power equipment cost, discount rate and inflation rate result in the largest changes in the NPC. The present study illustrates that the integrated renewable energy systems can be an effective and applicable approach for electrification in remote communities.

Acknowledgements
Funding for this work was provided by Natural Resources Canada through the Program of Energy Research and Development.

Author contributions
KQ: conceptualization, methodology, modeling, writing—original draft. EE: validation, writing—review and editing.

Declarations

Competing interests
The authors declare that they have no competing interests.

Received: 15 October 2023 Accepted: 21 February 2024
Published online: 12 March 2024

References

Afif, R. A., Ayed, Y., & Maaitah, O. N. (2022). Feasibility and optimal sizing analysis of hybrid renewable energy systems: A case study of Al-Karak, Jordan. *Renewable Energy, 204*, 229–249. https://doi.org/10.1016/j.renene.2022.12.109

Akinyele, D. O., & Rayudu, R. K. (2016). Techno-economic and life cycle environmental performance analyses of a solar photovoltaic microgrid system for developing countries. *Energy, 109*, 160–179. https://doi.org/10.1016/j.energy.2016.04.061

Almutairi, K., Hosseini, S. S., Hosseini, S. J., Mostafaeipour, A., Issakhov, A., & Techato, K. (2021). Use of a integrated wind-solar-diesel-battery energy system to power buildings in remote areas: A case study. *Sustainability, 13*, 8764. https://doi.org/10.3390/su13168764

Anoune, K., Bouya, M., Astito, A., & Abdellah, A. B. (2018). Sizing methods and optimization techniques for PV-wind based hybrid renewable energy system: A review. *Renewable and Sustainable Energy Reviews, 93*, 652–673. https://doi.org/10.1016/j.rser.2018.05.032

Baghaee, H. R., Mirsalim, M., Gharehpetian, G. B., & Talebi, H. A. (2016). Reliability/cost-based multi-objective Pareto optimal design of stand-alone wind/PV/FC generation microgrid system. *Energy, 115*, 1022–1041. https://doi.org/10.1016/j.energy.2016.09.007

Bagheri, M., Shirzadi, N., Bazdar, E., & Kennedy, C. A. (2018). Optimal planning of integrated renewable energy infrastructure for urban sustainability: Green Vancouver. *Renewable and Sustainable Energy Reviews, 95*, 254–264. https://doi.org/10.1016/j.rser.2018.07.037

Bahramara, S., Moghaddam, M. P., & Haghifam, M. R. (2016). Optimal planning of integrated renewable energy systems using HOMER: A review. *Renewable and Sustainable Energy Reviews, 62*, 609–620. https://doi.org/10.1016/j.rser.2016.05.039

Baneshi, M., & Hadianfard, F. (2016). Techno-economic feasibility of integrated diesel/PV/wind/battery electricity generation systems for non-residential large electricity consumers under southern Iran climate conditions. *Energy Conversion and Management, 127*, 233–244. https://doi.org/10.1016/j.enconman.2016.09.008

Bartolini, A., Carducci, F., Muñoz, C. B., & Comodi, G. (2020). Energy storage and multi energy systems in local energy communities with high renewable energy penetration. *Renewable Energy, 159*, 595–609. https://doi.org/10.1016/j.renene.2020.05.131

Branker, K., Pathak, M. J. M., & Pearce, J. M. (2011). A review of solar photovoltaic levelized cost of electricity. *Renewable and Sustainable Energy Reviews, 15*, 4470–4482. https://doi.org/10.1016/j.rser.2011.07.104

Chauhan, A., & Saini, R. P. (2016). Techno-economic optimization based approach for energy management of a stand-alone integrated renewable energy system for remote areas of India. *Energy, 94*, 138–156. https://doi.org/10.1016/j.energy.2015.10.136

Couto, N., Rouboa, A., Silva, V., Monteiro, E., & Bouziane, K. (2013). Influence of the biomass gasification processes on the final composition of syngas. *Energy Procedia, 36*, 596–606. https://doi.org/10.1016/j.egypro.2013.07.068

Das, I., & Cañizares, C. A. (2019). Renewable energy integration in diesel-based microgrids at the Canadian Arctic. *Proceedings of the IEEE, 107*(9), 1838–1856. https://doi.org/10.1109/JPROC.2019.2932743.
Dehshiri, H. S. S. (2022). A new application of multi criteria decision making in energy technology in traditional buildings: A case study of Isfahan. *Energy, 240*, 122814. https://doi.org/10.1016/j.energy.2021.122814
Diab, A. A. Z., Sultan, H. M., & Kuznetsov, O. N. (2020). Optimal sizing of hybrid solar/wind/hydroelectric pumped storage energy system in Egypt based on different meta-heuristic techniques. *Environmental Science and Pollution Research, 27*, 32318–32340. https://doi.org/10.1007/s11356-019-06566-0
Dolara, A. S., Leva, S., & Manzolini, G. (2015). Comparison of different physical models for PV power output prediction. *Solar Energy, 119*, 83–99. https://doi.org/10.1016/j.solener.2015.06.017
Government of Canada. (2011). Status of remote/off-grid communities in Canada. *Government of Canada*. https://doi.org/10.3390/su4081806
Hansen, M. O. L. (2007). *Aerodynamics of wind turbines* (2nd ed.). Routledge.
Hoff, T. E., & Perez, R. (2010). Quantifying PV power output variability. *Solar Energy, 84*, 1782–1793. https://doi.org/10.1016/j.solener.2010.07.003
Holdmann, G., Pride, D., Poelzer, G., Noble, B., & Walker, C. (2022). Critical pathways to renewable energy transitions in remote Alaska communities: A comparative analysis. *Energy Research & Social Science, 91*, 102712. https://doi.org/10.1016/j.erss.2022.102712
Holdmann, G. P., Wies, R. W., & Vandermeer, J. B. (2019). Renewable energy integration in Alaska's remote Islanded microgrids: Economic drivers, technical strategies, technological niche development, and policy implications. *Proceedings of the IEEE, 107*(9), 1820–1837. https://doi.org/10.1109/JPROC.2019.2932755
HOMER Energy. (2023). HOMER pro version 3.16.2 user manual. Retrieved December 20, 2023, from https://www.homerenergy.com
Hosseinalizadeh, R., Shakouri, G. H., Amalnick, M. S., & Taghipour, P. (2016). Economic sizing of a integrated (PV–WT–FC) renewable energy system (HRES) for stand-alone usages by an optimization-simulation model: Case study of Iran. *Renewable and Sustainable Energy Reviews, 54*, 139–150. https://doi.org/10.1016/j.rser.2015.09.046
IEC. (2021). Photovoltaic devices. Procedures for temperature and irradiance corrections to measured IV characteristics. IEC 60891. Retrieved November 10, 2023, from https://webstore.iec.ch/publication/61766
Jahangiri, M., Haghani, A., Mostafaeipour, A., Khosravi, A., & Raeisi, H. A. (2019). Assessment of solar-wind power plants in Afghanistan: A review. *Renewable and Sustainable Energy Reviews, 99*, 169–190. https://doi.org/10.1016/j.rser.2018.10.003
Kamaril, M. L., Isvand, H., & Nazari, M. A. (2020). Applications of multi-criteria decision-making (MCDM) methods in renewable energy development: A review. *Renewable Energy Research and Application, 1*, 47–54. https://doi.org/10.22044/rera.2020.8541.1006
Lovekin, D., & Heerema, D. (2019). *The true cost of energy in remote communities: Understanding diesel electricity generation terms and economics*. Pembina Institute. https://www.pembina.org/reports/diesel-cost-backgrounder-2019.pdf
Mahbaz, S. B., Dehghani-Sanij, A. R., Dusseault, M. B., & Nathwani, J. S. (2020). Enhanced and integrated geothermal systems for sustainable development of Canada's northern communities. *Sustainable Energy Technologies and Assessments, 37*, 100565. https://doi.org/10.1016/j.seta.2019.100565
McCallum, C. S., Kumar, N., Curry, R., McBride, K., & Doran, J. (2021). Renewable electricity generation for off grid remote communities; life cycle assessment study in Alaska, USA. *Applied Energy, 299*, 117325. https://doi.org/10.1016/j.apenergy.2021.117325
NASA. (2017). Surface meteorology and solar energy. Global data sets, Atmospheric Science Data Center. Retrieved November 10 2023, from https://asdc.larc.nasa.gov/project/SSE
Prabatha, T., Hager, J., Carneiro, B., Hewage, K., & Sadiq, R. (2020). Analyzing energy options for small-scale off-grid communities: A Canadian case study. *Journal of Cleaner Production, 249*, 119320. https://doi.org/10.1016/j.jclepro.2019.119320
Rahbar, K., Cha, C. C., & Zhang, R. (2018). Energy cooperation optimization in microgrids with renewable energy integration. *IEEE Transactions on Smart Grid, 9*, 1482–1493. https://doi.org/10.1109/TSG.2016.2600863
Sambor, D. J., Penn, H., & Jacobson, M. Z. (2023). Energy optimization of a food-energy-water microgrid living laboratory in Yukon, Canada. *Energy Nexus, 10*, 100200. https://doi.org/10.1016/j.nexus.2023.100200
Sameti, M., Kasaeian, A., & Astaraie, F. R. (2014). Simulation of a ZEB electrical balance with a integrated small wind/PV. *Sustain Energy Sustainable Energy, 2*(1), 5–11. https://doi.org/10.12691/rse-2-1-2
Sedghiyan, D., Ashouri, A., Maftouni, N., Xiong, Q., Rezaee, E., & Sadeghi, S. (2021). Prioritization of renewable energy resources in five climate zones in Iran using AHP, integrated AHP-TOPSIS and AHP-SAW methods. *Sustainable Energy Technologies and Assessments, 44*, 101045. https://doi.org/10.1016/j.seta.2021.101045
Shahzad, M. K., Zahid, A., Rashid, T., Rehan, M. A., Ali, M., & Ahmad, M. (2017). Techno-economic feasibility analysis of a solar-biomass off grid system for the electrification of remote rural areas in Pakistan using HOMER software. *Renewable Energy, 106*, 264–273. https://doi.org/10.1016/j.renene.2017.01.033
Shezan, S. A., Julai, S., Kibria, M. A., Ullah, K. R., Saidur, R., & Chong, W. T. (2016). Performance analysis of an off-grid wind-PV (photovoltaic)-diesel-battery integrated energy system feasible for remote areas. *Journal of Cleaner Production, 125*, 121–132. https://doi.org/10.1016/j.jclepro.2016.03.014
Singh, S., Singh, M., & Kaushik, S. C. (2016). Feasibility study of an islanded microgrid in rural area consisting of PV, wind, biomass and battery energy storage system. *Energy Conversion and Management, 128*, 178–190. https://doi.org/10.1016/j.enconman.2016.09.046
Sinha, S., & Chandel, S. S. (2014). Review of software tools for integrated renewable energy systems. *Renewable and Sustainable Energy Reviews, 32*, 192–205. https://doi.org/10.1016/j.rser.2014.01.035
Solomon, M. D., Heineken, W., Scheffler, M., & Birth, T. (2023). Energy conveyor belt—A detailed analysis of a new type of hydrokinetic device. *Energies, 16*, 2188. https://doi.org/10.3390/en16052188
Stringer, T., & Joanis, M. (2023). Decarbonizing Canada's remote microgrids. *Energy, 264*, 126287. https://doi.org/10.1016/j.energy.2022.126287
Tar, K. (2008). Some statistical characteristics of monthly average wind speed at various heights. *Renewable and Sustainable Energy Reviews, 12*(6), 1712–1724. https://doi.org/10.1016/j.rser.2007.01.014
Thirunavukkarasu, M., Sawle, Y., & Lala, H. (2023). A comprehensive review on optimization of hybrid renewable energy systems using various optimization techniques. *Renewable and Sustainable Energy Reviews, 176*, 113192. https://doi.org/10.1016/j.rser.2023.113192

Publisher's Note